Mathematical Dipoles are Adequate to Describe Realistic Generators of Human Brain Activity

JAN C. DE MUNCK, BOB W. VAN DIJK, AND HENK SPEKREIJSE

Abstract—**It is investigated whether a mathematical dipole description is adequate for the localization of brain activity on the basis of VEP's. Extended sources (dipole disks and dipole annuli) are simulated and fitted with a mathematical dipole. It is found that the deviation between the positions of the disks and annuli and the equivalent dipole is very small. Also the differences in the direction and amplitude may be neglected. The position of the extended source with respect to the electrode grid does not much influence these conclusions.**

I. Introduction

MOST mathematical models for the determination of the location, orientation, and strength of electrical brain activity from potential recordings at the scalp use the assumption that the cortical source can be described by a current dipole. Different volume conductor models have been proposed and compared like the homogeneous model [1], the three-sphere model [2], the four-sphere model [3], "realistic" models [4], and, recently, the anisotropic multisphere model [5]. Much attention has also been paid to the influence that deviating volume conductor model parameters have on the parameters that define an equivalent dipole [6], [7].

Since most of the cortex is layered and locally homogeneous, current flows radially through the cortical surface. Extended cortical sources can therefore likely be described by sheets with a homogeneous distribution of dipoles which are normally oriented to the sheet. Little attention, however, has been given to the assumption whether such an extended cortical generator can indeed be described by a single dipole.

The visual field is projected retinotopically to a number of cortical areas and generally a substantial part of the visual cortex will be activated in visually-evoked potential (VEP) studies. Subdural recordings from the Rhesus monkey have shown that even under stringent conditions to restrict stimulus field, eye movements, and stray light, the amount of activated cortical area is substantial [8]. Moreover, reduction of stimulus field size will always be at the cost of signal-to-noise ratio and thus will affect the accuracy of the location procedure.

Manuscript received November 9, 1987; revised June 13, 1988. The work of J. C. de Munck was supported by the Netherlands Organization for Scientific Research (N.W.O.) through the Foundation for Biophysics.

The authors are with the Department of Visual System Analysis, The Netherlands Ophthalmic Research Institute, 1100 AC Amsterdam-Zuidoost, The Netherlands.

IEEE Log Number 8823296.

To our knowledge Cuffin [9] is the only paper which analyzes the effect of source configuration on the parameters of an equivalent dipole. However, Cuffin used line sources and sheets with nonradial dipole distributions which we consider not to represent physiological sources adequately. Furthermore, Cuffin positioned the source always such that it was completely covered by the electrode grid, which is not realistic considering the occipital layout of the visual cortex.

The purpose of the present study is to investigate the influence of source extension on the position, orientation, and strength of an equivalent point dipole. We have simulated the potential fields of extended sources with disk- or annulus-like shapes, and we have calculated the equivalent dipoles for these potential fields. These fields and the dipole fields were calculated in the three-sphere volume conductor model (see Fig. 1) with the same model parameters as have been used by Ary and Klein [2] ($f_1 = 0.92$; $f_2 = 0.87$; $\xi = 0.0125$ where ξ is the ratio of the conductivity of the skull and the brain).

The choice of an "electrode grid" might influence the dependence of the equivalent dipole parameters on the dimensions of the source. With each electrode, two parameters (not three as every electrode is at the scalp) are chosen which influence the position of the equivalent dipole. The effects from the electrode grid will be the largest when a small number of electrodes is used, and when the source does not lie under the electrode grid. The latter is, for instance, the case when the source studied is "out of reach." An example are the lower parts of the striate and prestriate visual cortexes, which receive input from the upper visual half field; the heavy neck musculature hinders electrode placement above such sources. We used two different approaches to quantify the effect of the electrode grid: 1) we have simulated potential fields due to extended sources which are either right below the center of the electrode grid or at the border of the grid, and the equivalent dipoles for these two situations were determined and 2) we have calculated equivalent dipoles when all possible electrode positions are taken into account by integrating over the entire surface of the head; this is analogous to an infinite number of electrodes and yields the optimal equivalent dipole fit of the potential field of the extended source.

Some preliminary results of the latter simulations have been presented [10].

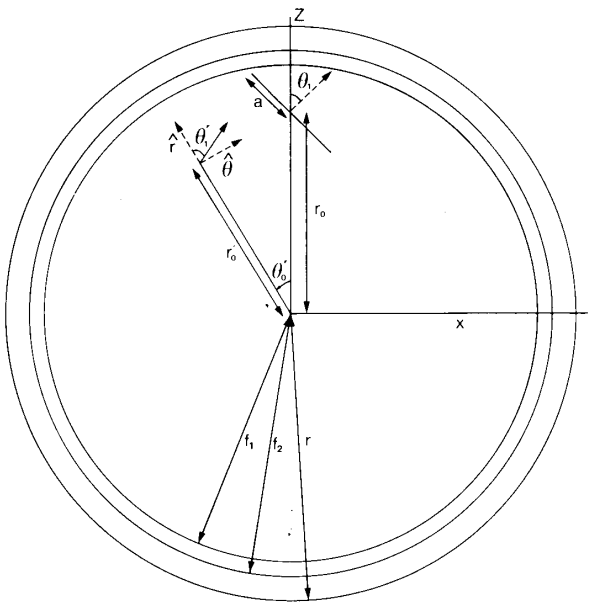

Fig. 1. Definition of the symbols. f_1 and f_2 denote the inner and the outer skull radius, respectively.

II. Methods

We define an equivalent dipole by the set of parameters $\boldsymbol{p}$ (three for position, and three for strength and orientation) for which the difference H between the potential distribution of the dipole [denoted by $V_p(\boldsymbol{x})$] and a given potential distribution is minimal. The equivalent dipole can thus be obtained by solving the equation

$$dH/d\boldsymbol{p} = 0. \tag{1}$$

A. Analytic Simulation

Equation (1) has been solved analytically [11], using spherical harmonics, for circle symmetry situations such as a dipole layer on a disk or annulus in a three-sphere volume conductor. The difference function $H(\boldsymbol{p})$ is found by integrating the difference between the dipole potential distribution $V_p(\boldsymbol{x})$ and the potential distribution due to the disk or annulus $V_L(\boldsymbol{x})$ over the entire outer surface of the head:

$$H(\boldsymbol{p}) = \oiint \left[V_L(\boldsymbol{x}) - V_p(\boldsymbol{x})\right]^2 d\boldsymbol{x}. \tag{2}$$

B. Discrete Simulation

In practice, potential values will only be recorded at a limited number of electrode positions and often with respect to a reference electrode. In that case, the difference function can be defined by

$$H(\boldsymbol{p}) = \sum_i \left[\left\{V_L(\boldsymbol{x}_i) - V_L(\text{ref})\right\} - \left\{V_p(\boldsymbol{x}_i) - V_p(\text{ref})\right\}\right]^2 \tag{3}$$

in which $\boldsymbol{x}_i$ denotes the position of the ith electrode and ref represents the position of the reference electrode. The values $V_L(\boldsymbol{x})$ were calculated by summation of the potential values due to a set of dipoles homogeneously distributed over the surface of the disk or annulus and radial to the surface of the dipole sheet (most times about 30 dipoles were used). The solution of (1) with $H(\boldsymbol{p})$ as in (3) was achieved with a computer program that follows the algorithm described by Powell [12].

C. Coordinate System

The position of the center of the extended source is given in polar coordinates r_0, θ_0, and ϕ_0, and the direction of the normal to the surface of the source in local polar coordinates θ_1 and ϕ_1. The size of the disk or annulus representing the source is specified by the radius a. The position of the equivalent dipole is given in the polar coordinates r_0', θ_0', and ϕ_0', and its direction in local polar coordinates θ_1' and ϕ_1' (see Fig. 1).

Since application of the results for VEP studies was one of the intents of the present study, the electrode grid was chosen on the occiput, covering θ values in the range 50–100°. Larger values would not be realistic considering the neck muscles. The coordinate system and the electrode grid used in the simulations are depicted in Figs. 2 and 3, respectively. An almost identical electrode grid is routinely used in our laboratory for dipole location measurements of VEP recording [13]. In the coordinate system of Fig. 2, the primary visual cortex lies at or close to the X axis at ϕ values below 10°. The prestriate cortexes lie between the second and third row of the electrode grid at ϕ values between −40 and −10° or between +10 and +40°. In the remainder of this text, angles will be expressed in degrees and the radius of the head will have unit length.

To describe the parameter deviation between the real source and the equivalent dipole, we have determined the following parameters:

—Depth deviation Δr_0, which is defined by

$$\Delta r_0 = r_0' - r_0. \tag{4}$$

—Amplitude deviation ΔA

$$\Delta A = (\text{Amp}' - \text{Amp})/\text{Amp}. \tag{5}$$

—The position error, which is defined as the angle between the vector pointing to the center of the extended source and the position vector of the equivalent dipole in degrees.

—The orientation error, which is defined as the angle between the vector normal to the surface of the extended source and the dipole vector.

In the Appendix, the position error and the orientation error are derived formally.

III. Results

A. Analytic Simulation

Since $H(\boldsymbol{p})$ is taken over the entire surface, (1) will be invariant for rotations around the center of the coordinate

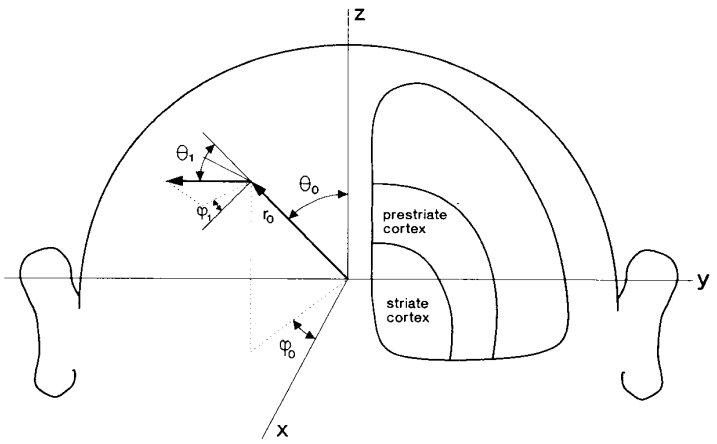

Fig. 2. The definition of the spherical coordinates with respect to the head. The positive x axis is through the inion, the y axis runs parallel to the line through both earholes and the positive x axis is through the top of the head. On the left side, it is shown where the striate and prestriate cortex are located with respect to this frame.

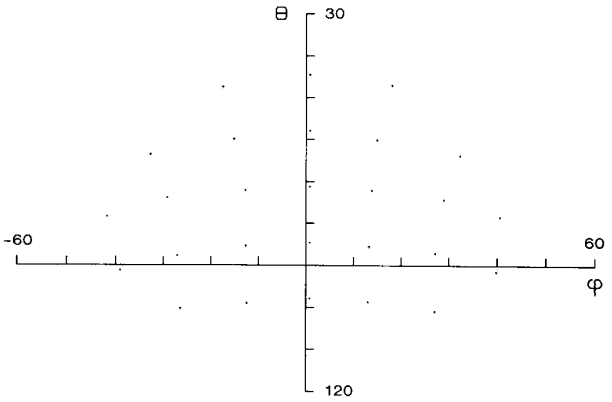

Fig. 3. The electrode grid. Every row is formed by measuring steps of 2.5 cm from the inion in a horizontal plane. The rows are 2.5 cm apart when measured from the inion over the head in a vertical plane.

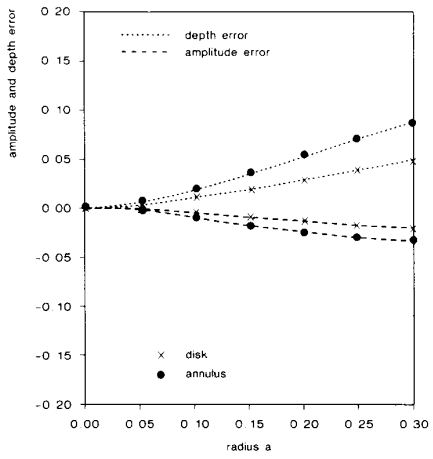

Fig. 4. Analytic simulation $\theta_1 = 0°$. The parameter deviations are plotted as function of a, which varies from 0 to 0.3. The deviation in the angles θ_1 and θ_0 are zero because of the symmetry present. The "stars" represent the disks and the "0"'s represent the annuli.

frame. For that reason, θ_0, ϕ_0, and ϕ_1 may be chosen to be zero without loss of generality. As a consequence, ϕ_1' and ϕ_0' will always be zero as well [11]. The remaining parameters have been so chosen that the disk or annulus always touches the outer surface of the compartment representing brain tissue. Results for disk-shaped sources are presented graphically in Figs. 4 and 5. In Fig. 4, the orientation of the disk was chosen parallel to the skull, i.e., $\theta_1 = 0°$, and depth of the disk and its size were varied. In Fig. 5, the size was fixed at $a = 0.3$ while the orientation θ_1 and the depth were varied. From Figs. 4 and 5 it is evident that even for the most extended source the errors in amplitude, depth, position, and orientation are very small; the depth deviation is less than 0.05 of the radius of the head for a disk with a radius of 30 percent of the head.

Results for annularly-shaped sources are also depicted in Fig. 4. We have fixed θ_1 at 0° and have varied the depth and size of the annulus. The errors are larger than found for disk-shaped sources, yet they are still smaller than 0.1 for an annulus with radius 0.3.

B. Discrete Simulation

1) Striate Cortex: In discrete simulation, the function $H(\boldsymbol{p})$ will not be invariant for rotations around the center of the coordinate frame. Realistic positions have been chosen for the center of the source: either close to the center of the electrode grid, i.e., $\phi_0 = 0°$ and $\theta_0 = 80°$ or just under the lower border of the electrode grid, i.e., at $\phi_0 = 0°$ and $\theta_0 = 100°$. These positions correspond to, respectively, the projection of the lower visual half field and the upper visual half field in the striate visual cortex. As for the analytic simulations the sources have been so chosen that the edge of the disk or annulus just

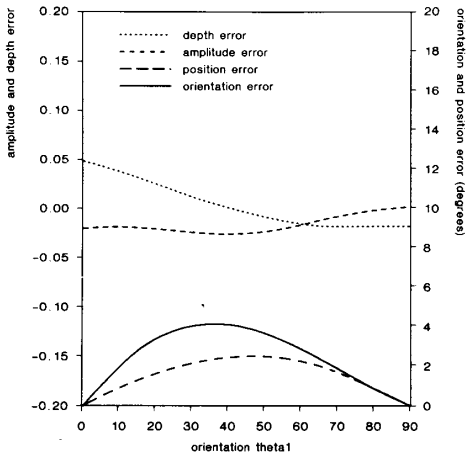

Fig. 5. Analytic simulation, $a = 0.3$. The parameter deviations are plotted as function θ_1.

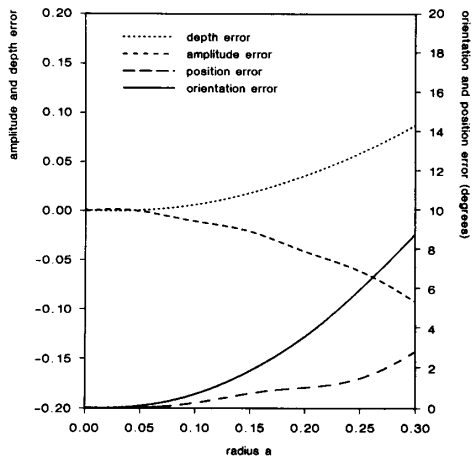

Fig. 6. Discrete simulation of the projection of the lower visual field. $\theta_0 = 80°$, $\phi_0 = \theta_1 = \phi_1 = 0°$, a varies.

touches the outer surface of the compartment representing brain tissue.

The discrete simulation results for disk-shaped sources located right below the center of the electrode grid are presented in Figs. 6 and 7. In Fig. 6, the parameters θ_1 and ϕ_1 have been chosen equal to 0° since at the projection from the fovea the cortical field runs parallel to the scalp. As can be seen, the errors in position, orientation, and strength are of the same order of magnitude as found for the analytic simulations. This indicates that the number of electrodes and the electrode spacing used in our laboratory routinely are sufficient for localization procedures.

In the second set of simulations for lower visual field stimulation of striate cortex, we have studied the effect of a cortical generator which lies partly at the medial wall of the hemisphere. This corresponds to stimulation of the peripheral visual field. We have chosen a fixed value for the extension $a = 0.3$ and $\phi_1 = -90°$, while we have varied the depth r_0 and the orientation θ_1. The results are presented in Fig. 7. As can be seen, the errors in depth and amplitude are smaller than for purely radial sources, while the errors in position and orientation are slightly larger. The largest error in the orientation is still smaller than 12°.

The results for disk-shaped sources located at the lower border of area 17 are presented in Fig. (8). At this projection site, the cortical surface bends strongly inward. For that reason, we have varied the parameters θ_1 and r_o instead of a and r_0. The size of the disk was chosen equal to 0.3 the parameter ϕ_1 equal to 0°. Again, we have chosen the parameters such that the disk just touches the outer surface of the compartment representing brain tissue. As expected, the errors in depth and strength are larger than for the projection of the lower visual field. The largest error found in the amplitude of the dipole is a 12.5 percent underestimation, when the disk is oriented radially. If the disk is tangentially oriented, a 7 percent underestimation of the amplitude occurs. The errors in position and ori-

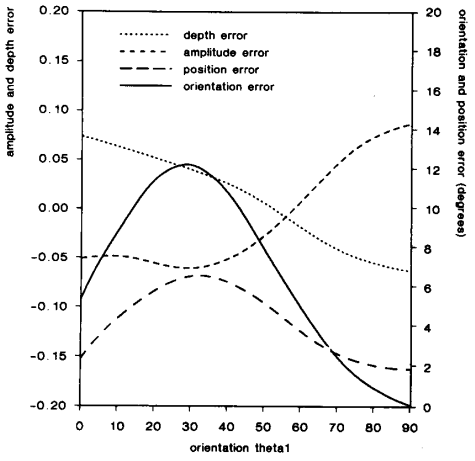

Fig. 7. Discrete simulation of the projection of the lower visual field. $\theta_0 = 80°$, $\phi_0 = 0°$ $\phi_1 = -90°$, $a = 0.3$, θ_1 varies.

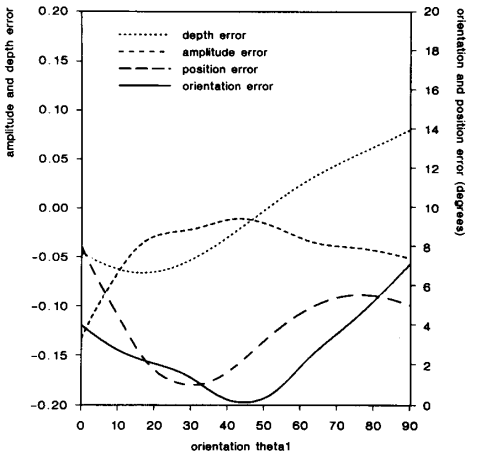

Fig. 8. Discrete simulation of the projection of the upper visual field. $\theta_0 = 100°$, $\phi_0 = \phi_1 = 0°$, $a = 0.3$, θ_1 varies.

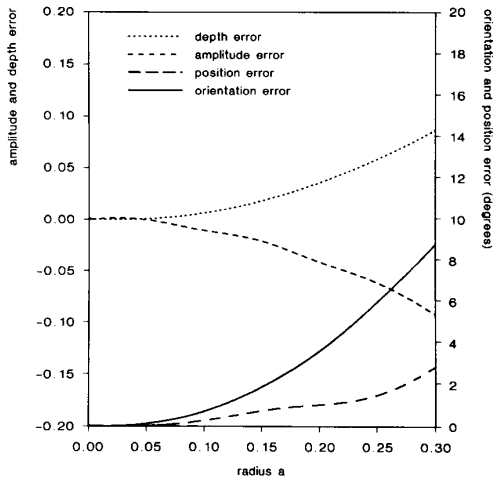

Fig. 9. Discrete simulation of prestriate cortex. $\theta_0 = 75°$, $\phi_0 = 20°$, $\theta_1 = \phi_1 = 0$, a varies.

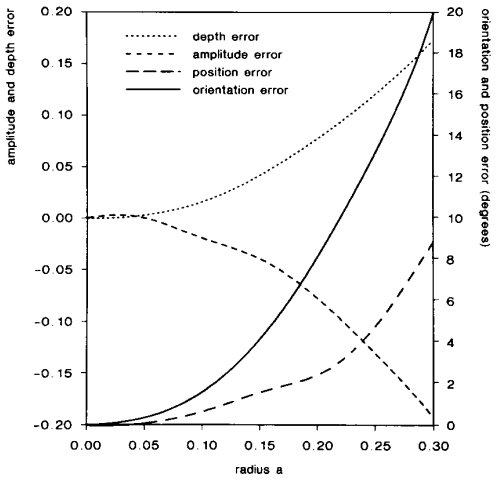

Fig. 10. As in Fig. 9, but now the extended source consists of a dipole ring.

entation are not much larger than for the lower visual field simulation.

2) Prestriate Cortex: We have mimicked an extended prestriate cortical source in the right hemisphere by a disk-shaped source at $\theta_o = 75°$ and $\phi_o = 20°$. We have varied the size and depth r_o such that each disk just touches the outer surface of the volume conductor compartment which represents the brain. The orientation of the disk was chosen parallel to the skull, which is the most likely orientation considering the anatomy of the prestriate cortex. Results are given in Fig. 9. Errors are approximately of the same magnitude as for the projection of lower fovea on the striate cortex.

3) Annular Shaped Sources: To obtain a worst case estimate of the effects of the modeling errors involved, we have used annular-shaped instead of disk-shaped sources. These annuli were chosen in the prestriate region. Results are shown in Fig. 10; the parameters were chosen as in

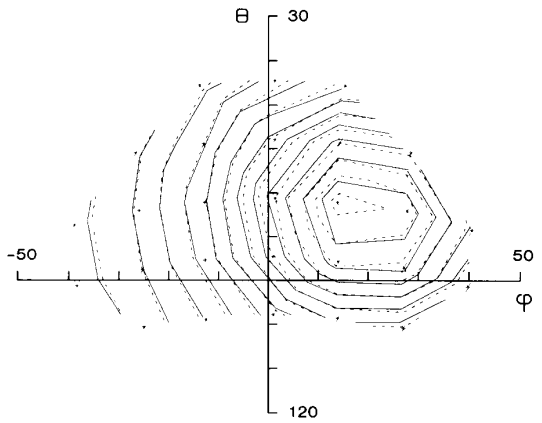

Fig. 11. Equipotential lines of the potential distribution on the scalp. Continuous lines: annulus source (parameters $a = 0.3$, $\theta_0 = 75°$, $\phi_0 = 20°$, $\theta_1 = \theta_1 = 0°$); broken lines: equivalent dipole.

Fig. 9. As expected, the errors are larger, yet they can be considered small when compared to the errors that deviating volume conductances can introduce [6].

4) Contour Plots: Fig. 11 shows two sets of equipotential maps obtained by linear triangular extrapolation on the electrode grid. The map, represented by the continuous lines, belongs to a simulated extended annularly-shaped source with radius 0.3, parallel to the skull, immediately underneath the center of the electrode grid. The other map, represented by dashed lines, belongs to the equivalent dipole field. From Fig. 11 it is evident, that not only the location and amplitude are adequately described by a single equivalent dipole, but that also the potential fields due to both types of sources are highly similar.

IV. Discussion

The results of this simulation study show clearly that the assumption of electric brain activity represented by an equivalent point dipole does not yield large errors in the position, orientation, and strength parameters.

The small deviations found are not specific for the volume conductor model used or the integrative properties of the skull. For the analytic simulations, we have observed that the errors obtained when the head is modeled by a homogeneous sphere are almost identical.

Although the depth deviations are small, they are systematic. For $\theta_1 = 0°$, the equivalent dipole always lies deeper than the dipole layer and for $\theta_1 = 90°$ the location is more superficial. This could be expected because for $\theta_1 = 0°$ the simulated potential distribution on the scalp will be broad, which corresponds to a relatively deep dipole. On the other hand, for $\theta_1 = 90°$, the dipoles in the sheet which are nearest to the scalp will contribute more to the scalp potential distribution than the deeper dipoles. Therefore, the equivalent dipole will be shallower than the gravity point of the sheet. It is striking, however, that these effects are small.

It should be noticed that in source localization studies

the visual cortex is most sensitive to modeling errors. It lies very close to the skull and a large part of the visual cortex is covered by the neck musculature. The deeper the cortical sources lie, the less prone to modeling errors of the type discussed in this paper they will be. Our data show, however, that even in an unfavorable situation (a superficial annular-shaped source) the errors are not large at all.

This study intended to analyze the consequences of modeling a realistic source by a dipole. It will be evident that realistic sources are not identical to disks or annuli. However, we believe that the conclusions drawn in this paper may be generalized. For a homogeneous source layer, only the contour of the source determines the resulting potential field; therefore, our data are not restricted to disks or annuli but also cover other sources with a circular contour.

We may assume that our data cover more than the physiological range of sizes of active regions. When the entire visual cortex would be homogeneously active, the size of the active layer in human would be 2300 mm^2. This is equivalent to a radius of approximately 25 percent of the head radius.

A direct conclusion from the present study is that it is not necessary to restrict the activated cortex to a small region for obtaining a good description by one equivalent dipole. Even when the cortical source is large and when the source is not entirely covered by the electrode grid, this will not result in large errors. Of course a malalignment or a strongly restricted stimulus field will have consequences for the amplitude of the recorded signal and thus on the accuracy of the localization procedure.

On the other hand, the data make clear that it will not be possible in practice to estimate the size of the activated cortical region even when the depth and the strength of the cortical source are known precisely. Not only are the parameters of the equivalent dipole accurately estimated, also the obtained potential field over the scalp upon a single dipole mimics closely the potential field due to an extended source (see Fig. 11). To determine the form and size of a cortical source, subdural recordings or current source density techniques seem indicated.

Appendix A

The error in position is defined as the angle ω_p between the position vectors $\boldsymbol{x}_0$ and $\boldsymbol{x}_0'$ of the extended source and the equivalent dipole, respectively. In a formula

$$\cos \omega_p = \sin \theta_0 \sin \theta_0' \cos (\phi_0 - \phi_0') + \cos \theta_0 \cos \theta_0'. \tag{A.1}$$

The determination of the error in orientation ω_o is somewhat more involved because the direction vectors $\boldsymbol{x}_1$ and $\boldsymbol{x}_1'$ are defined in different coordinate frames. First, $\boldsymbol{x}_0'$ is rotated such that $\boldsymbol{x}_0'$ and $\boldsymbol{x}_0$ are on the same axis and then the inverse of this rotation is applied on $\boldsymbol{x}_1'$. The angle between the result and $\boldsymbol{x}_1$ is the required orientation error.

The rotation to be found is the rotation $R(\boldsymbol{n}, \omega_p)$ about the axis $\boldsymbol{n}$ over the angle ω_p. For $\boldsymbol{n}$ we find

$$\boldsymbol{n} = \frac{\boldsymbol{x}_0' \hat{} \boldsymbol{x}_0}{|\boldsymbol{x}_0' \hat{} \boldsymbol{x}_0|} \equiv \begin{pmatrix} \sin \theta_n & \cos \phi_n \\ \sin \theta_n & \sin \phi_n \\ \cos \theta_n & \end{pmatrix} \tag{A.2}$$

where $\hat{}$ is the cross product.

We can write for $R(\boldsymbol{n}, \omega_p)$

$$R(\boldsymbol{n}, \omega_p) = R_{nz} R(z, \omega_p) R_{nz}^{-1} \tag{A.3}$$

where R_{nz}^{-1} is a rotation which depicts the $\boldsymbol{n}$ axis on the z axis. So we find ω_o from

$$r_1 r_1' \cos (\omega_o) = \left(R_{nz} R^{-1}(z, \omega_p) R_{nz}^{-1} \boldsymbol{x}_1'\right) \cdot \boldsymbol{x}_1 \tag{A.4}$$

where $\cdot$ denotes the inner product.

The matrices R_{nz} and $R(z, \omega_p)$ are given by

$$R_{nz} = \begin{pmatrix} \cos \theta_n \cos \phi_n & -\sin \phi_n & \sin \theta_n \cos \phi_n \\ \cos \theta_n \sin \phi_n & \cos \phi_n & \sin \theta_n \sin \phi_n \\ -\sin \theta_n & 0 & \cos \theta_n \end{pmatrix} \tag{A.5}$$

$$R(z, \omega_p) = \begin{pmatrix} \cos \omega_p & -\sin \omega_p & 0 \\ \sin \omega_p & \cos \omega_p & 0 \\ 0 & 0 & 1 \end{pmatrix}. \tag{A.6}$$

References

[1] E. Frank, "Electric potential produced by two point current sources in a homogeneous conducting sphere," *J. Appl. Phys.*, vol. 23, no. 11, pp. 1225-1228, 1952.

[2] J. P. Ary, S. A. Klein, and D. H. Fender, "Location of sources of evoked scalp potentials: Correction for skull and scalp thickness," *IEEE Trans. Biomed. Eng.*, vol. BME-28, pp. 447-452, 1981.

[3] R. S. Hosek, A. Sances, Jr., R. W. Jodat, and S. J. Larson, "The contributions of intracerebral currents to the EEG and evoked potentials," *IEEE Trans. Biomed. Eng.*, vol. BME-25, pp. 405-413, 1978.

[4] R. C. Barr, M. Ramsey, III, and M. S. Spach, "Relating epicardial to body surface potential distributions by means of transfer coefficients based on geometry measurements," *IEEE Trans. Biomed. Eng.*, vol. BME-24, pp. 1-11, 1977.

[5] J. C. de Munck, "The potential distribution in a layered anisotropic spheroidal volume conductor," *J. Appl. Phys.*, vol. 64, no. 2, pp. 464-470, 1988.

[6] C. J. Stok, "The influence of model parameters on EEG/MEG single dipole source estimation," *IEEE Trans. Biomed. Eng.*, vol. BME-34, pp. 289-296, 1987.

[7] J. C. de Munck, unpublished.

[8] B. v. Dijk, G. Dagnelie, and H. Spekreijse, "Pattern responses from monkey primary visual cortex: Retinotopic map and receptive field properties," presented at 16th Ann. Meet. Soc. Neurosci., Nov. 1986.

[9] B. N. Cuffin, "A comparison of moving dipole inverse solutions using EEG's and MEG's," *IEEE Trans. Biomed. Eng.*, vol. BME-32, pp. 905-910, 1985.

[10] J. C. de Munck and H. Spekreijse, "The effect of source extension on the location and components of the equivalent dipole," *Topographic Brain Mapping of EEG and Evoked Potentials*, K. Maurer, Ed. New York: Springer-Verlag, 1988.

[11] J. C. de Munck, B. W. van Dijk, and H. Spekreijse, "An analytic method to determine the effect of source modeling errors on the apparent location and direction of biological sources," *J. Appl. Phys.*, vol. 63, no. 3, pp. 944-956, 1988.

[12] M. J. D. Powell, "An efficient method for finding the minimum of a function of several variables without calculating derivatives," *Comput. J.*, vol. 7, pp. 155-162, 1964.

[13] J. Maier, G. Dagnelie, H. Spekreijse, and B. W. van Dijk, "Principal components analysis for source localization of VEP's in man," *Vision Res.*, vol. 27, no. 2, pp. 165-177, 1987.

Jan C. de Munck received the physics degree from the University of Amsterdam, Amsterdam, The Netherlands, in 1985. His masters thesis dealt with the theory of directional hearing in code.

Since 1985 he has been with the Netherlands Ophthalmic Research Institute. He is working on his Ph.D. dissertation on the mathematical physical theory of EEG and VEP. He also is interested in the mechanism of accommodation.

Bob W. van Dijk received the physics and Ph.D. degrees from the University of Amsterdam, Amsterdam, The Netherlands, in 1985. The subject of his thesis was color coding in carp retina.

Since 1985 he has been with the Netherlands Ophthalmic Research Institute as Fellow of the Netherlands Organization for Scientific Research (NWO) through the Huygens program. His current research interests include electrophysiology of the central visual system in mammals. He participates in studies employing single cell physiology and in VEP-source localization studies.

Dr. Van Dijk is the recipient of the C.&C. Huygens award.

Henk Spekreijse received the physics degree from the Technological University of Delft, Delft, The Netherlands, and the Ph.D. degree from the University of Amsterdam, Amsterdam, The Netherlands.

He is Professor in visual system analysis at the Laboratory of Medical Physics, University of Amsterdam, and Director of research at the Netherlands Ophthalmic Research Institute.